Vol. **112** (2007) *ACTA PHYSICA POLONICA A* No. 6

Proceedings of the Workshop on Smoothing and Characterization of Magnetic Films...

Layer and Interface Structure of CoFe/Ru Multilayers

A.T.G. Pym[a], A. Lamperti[a], S. Cardoso[b], P.P. Freitas[b] and B.K. Tanner[a]

[a]Department of Physics, Durham University
South Road, Durham DH1 3LE UK
[b]INESC-MN, Rua Alves Redol 9, 1000-029 Lisboa, Portugal

Grazing incidence X-ray scattering measurements have been performed to probe the structure of CoFe/Ru layers and their interfaces. It was found that the interface width increased approximately linearly with the layer number from the substrate in a multilayer and that a substantial asymmetry existed between the width of CoFe/Ru and Ru/CoFe interfaces. By co--minimizing both the specular and diffuse scatter with that simulated from a model structure, the topological roughness amplitude was determined to be comparable to the intermixing interface width.

PACS numbers: 61.10.Kw, 68.65.Ac, 68.35.Ct, 75.50.Kj, 85.75.Dd, 85.70.Ay

1. Introduction

In fabrication of magnetic spin valves and magnetic tunnel junctions (MTJ), ruthenium is extensively used as a means of coupling antiferromagnetically the magnetization in two ferromagnetic layers. Elemental cobalt has a high magnetostriction, which makes its use as an electrode in spintronic devices unsatisfactory. However, by alloying it with iron this is dramatically reduced and an 80%Co20%Fe composition is very commonly used. Further, although Co and Ru are miscible, when cobalt is alloyed with iron the chemical affinity between the two reduces the miscibility with ruthenium [1] and the interfaces are expected to be relatively sharp.

The stability of the interface structure of sputtered $Ru/Co_{80}Fe_{20}$ layers during high temperature annealing has been studied recently [2] using grazing incidence X-ray scattering and interfaces have been shown to be stable up to at least 400°C. In this paper, we examine the interface structure of $Ru/Co_{80}Fe_{20}$ multilayers in more detail.

2. Experimental method

High resolution grazing incidence X-ray scattering measurements were made on $[Co_{80}Fe_{20}(30\ Å)/Ru(8\ Å)]_{13}/Co_{80}Fe_{20}(30\ Å)/Ru(30\ Å)$ multilayers grown at INESC by ion beam deposition on Si/Al_2O_3 in a Nordiko3000 system [3]. Experiments were performed at the station 2.3 of the Daresbury SRS synchrotron radiation source at X-ray wavelength 1.3 Å. All measurements were made at room temperature. In specular scattering, taken under conditions where the incident and exit beam angles are equal with respect to the surface, the momentum transfer vector is oriented perpendicular to the surface and thus the data contain no information on the in-plane structure of the material. Topological roughness and chemical intermixing across an interface cannot be distinguished. Diffuse scatter measurements are necessary to differentiate these two components to the interface width and determine the characteristic length scale of the topological roughness. Two types of measurement of the diffuse scatter were performed; the first being off-specular scans coupled in the ratio of 1:2 between sample and detector as for specular scattering, but with the sample displaced a small amount from the specular condition. This longitudinal scan in reciprocal space probes the diffuse scatter close to the forward direction and can be used both to determine the degree of conformality of the interface roughness in a multilayer and to determine the true specular scatter, the forward diffuse scatter having been subtracted. The second type of scan is also known as a rocking curve and is a measurement at fixed scattering angle of the X-ray scatter as a function of the angle of incidence on the sample. It is a transverse scan in reciprocal space. A detailed fitting of both specular and diffuse scatter data to a model structure was done using the REFS code, supplied by Bede X-ray Metrology [4]. This uses a fractal model of interfaces within the distorted wave Born approximation, the key parameters being in-plane correlation length ξ, r.m.s. roughness σ, chemical interface width Σ, and Hurst fractal parameter h, in addition to the thickness and composition of the layers themselves. For a multilayer, the model also includes an out-of-plane correlation length ζ, which describes the conformality of the roughness of successive layers through the multilayer stack.

3. Results

The specular scatter from a typical multilayer is shown in Fig. 1. Above the 2nd Bragg peak, the Kiessig fringes disappear, and simulation shows that this is indicative of a structure where the interface widths either systematically increase or decrease through the stack. Despite the robustness of the genetic algorithm in the fitting engine of the Bede REFS code, it was not possible to obtain a fit with a low error function [4] to all the Bragg peaks with constant interface widths in the repeated bi-layer stack. However, as evident in Fig. 1, a very good fit can be obtained when the layer is split up into three sub-stacks with almost identical layer thickness but significantly different interface width. This is sufficient to allow for

dispersion in the sample structure and accounts for the Bragg peak broadening at higher angles. The parameters which best fitted the data are given in Table.

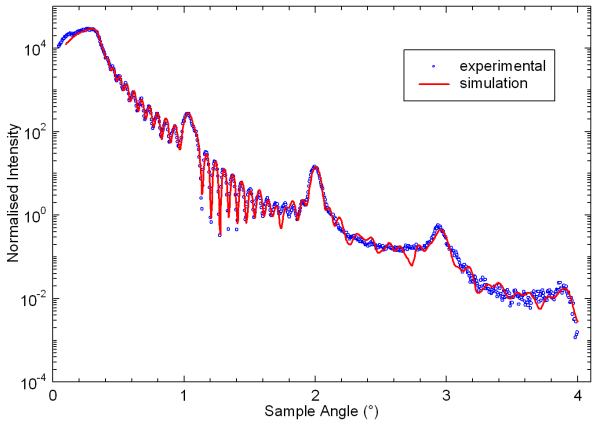

Fig. 1. True specular scatter (measured specular minus the forward off-specular scatter) as a function of incidence angle. The solid line is the best fit to the simulation from the model given in Table.

TABLE

Model structure deduced from the best fit to the scattering data. The multilayer has been split into three separate repeated structures to allow the evolution of the interface width as the sample has grown.

Layer		Material	Thickness (Å)	Top interface width (Å)	Roughness (Å)	Grading (Å)
29		RuO_2	1.2±2	6.6±0.9	5	4.3
28		Ru	26.5±2	10.6±4	5	9.3
27		$Co_{0.8}Fe_{0.2}$	28.6±1	6.2±0.6	5	3.6
17–26	×5	Ru	6.7±4	4.8±0.4	3	3.8
		$Co_{0.8}Fe_{0.2}$	30.9±4	6.7±2	5	4.5
9–16	×4	Ru	6.8±1	3.5±0.2	3	1.9
		$Co_{0.8}Fe_{0.2}$	30.9±1	5.4±0.8	4	3.6
1–8	×4	Ru	6.9±0.3	2.9±0.2	1.5	2.5
		$Co_{0.8}Fe_{0.2}$	30.8±0.3	3.8±0.3	1.5	3.5
Thick buffer		Al_20_3	∞	2.6±0.1	1.5	2.1

The parameters in Table were used to fit the diffuse scatter. From the magnitude of the diffuse scatter relative to the specular scatter, the topological

roughness and chemical intermixing can be distinguished. The distribution of the scatter with angle in the off-specular and rocking curve scans (Fig. 2) depends on the in-plane correlation length and the fractal parameter. A low value of ξ results in a very flat distribution of the scatter with angle in the rocking curve, as illustrated in Fig. 2b. By finding a single set of parameters that gave a good fit to both specular and diffuse scatter, we determined $\xi = 140 \pm 30$ Å and $h = 0.7 \pm 0.3$. The strong Bragg peaks in the off-specular scan (Fig. 2a) is indicative of a high degree of conformality in the roughness and a value of $\zeta = 300 \pm 100$ Å gave a good fit to the curve.

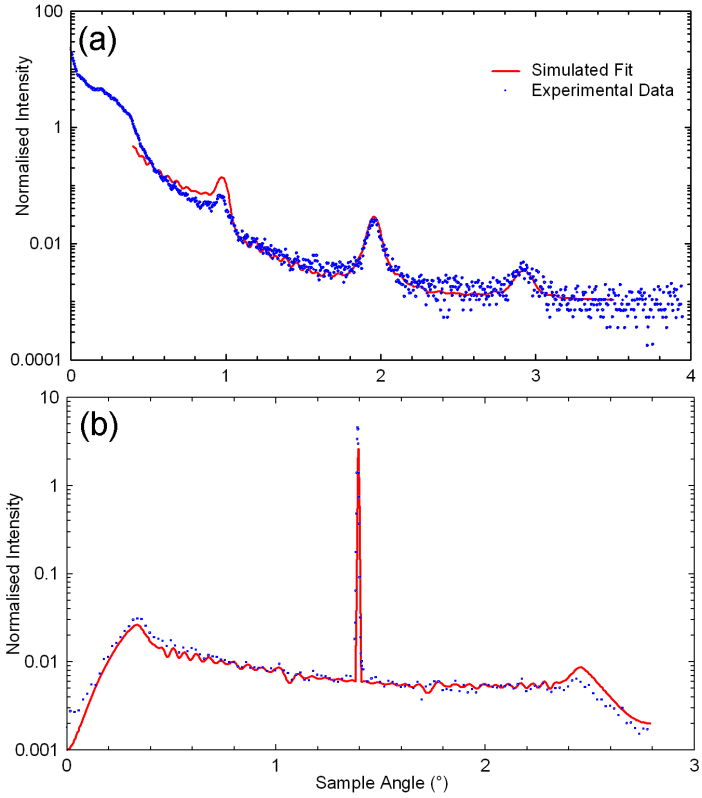

Fig. 2. (a) Off-specular coupled scan probing the forward diffuse scatter; the presence of three Bragg peaks in the diffuse scatter indicates a high degree of conformality in the roughness. (b) Rocking curve (transverse scan in reciprocal space) at a scattering angle of 2.79°. The solid line is the simulation using the parameters deduced from the fit to (a).

The asymmetry in the plot arises from the geometrical correction within the code for the beam "footprint", which is the change in illuminated area with incidence angle.

4. Discussion

Plotting the interface width recorded in Table graphically brings out the increase in interface width as a function of layer number. Only by inclusion of a significantly different roughness value at the Ru/CoFe and CoFe/Ru interfaces could a satisfactory fit to the data be obtained. Alternating roughness or interface width in multilayers has been known for a long time in semiconductor systems such as GaAs/AlAs [5], $Al_xGa_{1-x}As$/AlAs and Ge_xSi_{1-x}/Si [6]. The fractional variation is similar for both types of interface and throughout the growth, the Ru on CoFe interface is wider than the CoFe on Ru interface. In order to fit the diffuse scatter, the topological roughness had to be modelled as increasing with layer number but the data are not sufficiently sensitive to enable the separation of the topological roughness of the two interfaces. The best fit is found by assuming that the chemical width of the two interfaces differs (Table). Such an asymmetry in the width of intermixing in sputtered layers of aluminium on transition metals and vice versa was found by Buchanan et al. [7]. A similar asymmetry in interface width was found by Bigault et al. [8] in Ni/Au multilayers and Luo et al. [9] in NiFe/Cu multilayers, both using anomalous X-ray scattering. Bigault et al. suggested that that dynamical (out-of-equilibrium) segregation driven by the growth front probably determines the intermixing length and gives rise to the asymmetry.

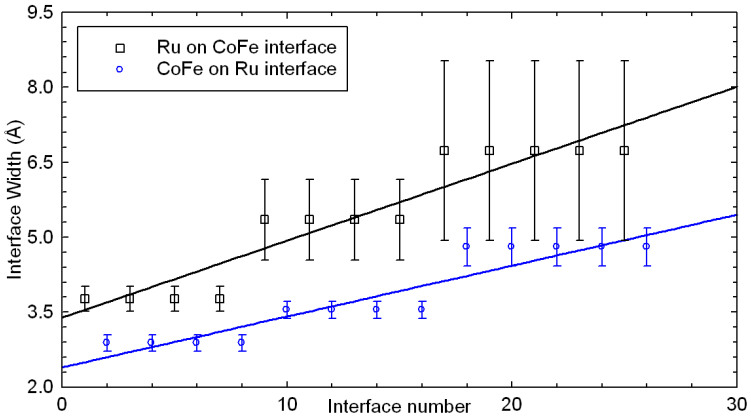

Fig. 3. Interface width as a function of interface number, counting upwards from the substrate.

As with most sputtered samples, the in-plane correlation length is quite short and corresponds to a typical grain size. The fractal parameter h can vary between 0, when the interface is three-dimensional in character, to 1, when the interface is of a two-dimensional nature. The high value of h found in these data indicates that the structure is predominantly two-dimensional, consistent with the relatively high degree of chemical intermixing.

In conclusion, we have shown that the interface structure in Ru/CoFe and CoFe/Ru interfaces differ and that the roughness and intermixing of both types of interface increases as more layers are deposited. While an increase in topological roughness amplitude is expected [10] for all growth models that show scaling behaviour [11], such as the Edwards-Wilkinson [12], KPZ [13] and TAB [14] models, the origin of the increase in intermixing width with layer repeat number is not clear.

Acknowledgments

The authors thank Dr Tony Bell of Daresbury Laboratory for technical support in the use of station 2.3 at the SRS. Financial support came from the UK Engineering and Physical Sciences Research Council and through the European Community's Marie Curie actions (Research Training Networks) under contract MRTN-CT-2003-504462, ULTRASMOOTH.

References

[1] J. Kaspar, D.B. Salahub, *J. Phys. F, Met. Phys.* **13**, 311 (1983).

[2] A.T.G. Pym, A. Lamperti, S. Cardoso, P.P. Freitas, B.K. Tanner, *Superlatt. Microstruct.* **41**, 122 (2007).

[3] S. Cardoso, V. Gehanno, R. Ferreira, P.P. Freitas, *IEEE Trans. Magn.* **35**, 2952 (1999).

[4] M. Wormington, K.M. Matney, C. Panacione, D.K. Bowen, *Philos. Trans. R. Soc. Lond. A* **357**, 2827 (1999).

[5] J. Berhend, M. Wassermeier, W. Braun, P. Krispin, K.H. Ploog, *J. Cryst. Growth* **175**, 178 (1997).

[6] M.K. Sanyal, A. Dhatta, S. Banerjee, A.K. Srivastava, B.M. Arora, S. Kanakaraju, S. Mohan, *J. Synchr. Radiat.* **4**, 185 (1997).

[7] J.D.R. Buchanan, T.P.A. Hase, B.K. Tanner, P.J. Chen, L. Gan, C.J. Powell, W.F. Egelhoff Jr., *Phys. Rev. B* **66**, 1044271 (2002).

[8] T. Bigault, F. Bocquet, S. Labat, O. Thomas, H. Renevier, *Phys. Rev B* **64**, 125414 (2001).

[9] G.M. Luo, Z.H. Mai, T.P.A. Hase, B.D. Fulthorpe, B.K. Tanner, C.H. Marrows, B.J. Hickey, *Phys. Rev. B* **64**, 2454041 (2001).

[10] F. Family, T. Vicsek, *Dynamics of Fractal Surfaces*, World Scientific, Singapore 1991.

[11] T. Salditt, T.H. Metzger, J. Peisl, *Phys. Rev. Lett.* **73**, 2228 (1994).

[12] S.F. Edwards, D.R. Wilkinson, *Proc. R. Soc. Lond. A* **381**, 1759 (1982).

[13] M. Kardar, G. Parisi, Y.-C. Zhang, *Phys. Rev. Lett.* **56**, 889 (1986).

[14] C. Tang, S. Alexander, R. Bruinsma, *Phys. Rev. Lett.* **64**, 772 (1990).